Raft River EGS Project: A GIS-Centric Review of Geology

Gregory D. Nash and Joseph N. Moore

Energy & Geoscience Institute at the University of Utah

Keywords

Raft River thermal anomaly, Raft River geology, GIS, geographic information systems, Raft River EGS, enhanced geothermal systems, Raft River faults

ABSTRACT

The Raft River thermal anomaly is located on the northern margin of the Great Basin. This area has undergone numerous studies due its juxtaposition with the Raft River and Albion metamorphic core complexes, associated low-angle detachment faults, and the presence of the thermal anomaly. Miocene movement along the Raft River detachment displaced a large mass of Paleozoic and Mesozoic rock about 24 km to the east unroofing the shear zone and creating the Raft River Valley. The rocks in the Raft River detachment footwall/shear zone are Archean and Proterozoic in age and are overlain by late Miocene/Pliocene ash-flow tuff, tuffaceous sediments, rhyolite, and mixed Quaternary sediments.

Work described here supports the DOE/U.S. Geothermal, Inc. supported Raft River EGS project which is aimed toward improving permeability in well RRG-9. A GIS data suite was developed from historical data and new data produced by this study to help underpin this project. The GIS includes well survey, lithologic, mineralogic, and geophysical data that were incorporated from disparate datasets ranging from scanned images to tabular data in spreadsheets. This data has been visualized and analyzed using GIS-based tools to help build a better understanding of the study area geology. This includes a possible structural explanation of ground water/geothermal fluid compartmentalization.

Introduction

The Raft River thermal anomaly is located in the Raft River Valley, Idaho, a north-trending Cenozoic basin on the northern edge of the Great Basin, just west of the Central Rocky Mountains, near its transition into the Snake River Plane. It lies ~11.5 km north of the Raft River Range (Fig. 1) at an elevation of approximately 4800 ft MSL.

U.S. Geothermal owns or leases approximately 8.2 square miles of land over the Raft River thermal anomaly. A 13 MW net capacity power plant is currently in operation at the site.

This study is in support of the Raft River Enhanced Geothermal System (EGS) project, a cooperative effort between the U. S. Department of Energy; the Energy & Geoscience Institute/University of Utah; U.S. Geothermal Inc., Geothermal Resources Group; and Apex HiPoint Reservoir Engineering. Additional support is also provided by Lawrence Berkeley

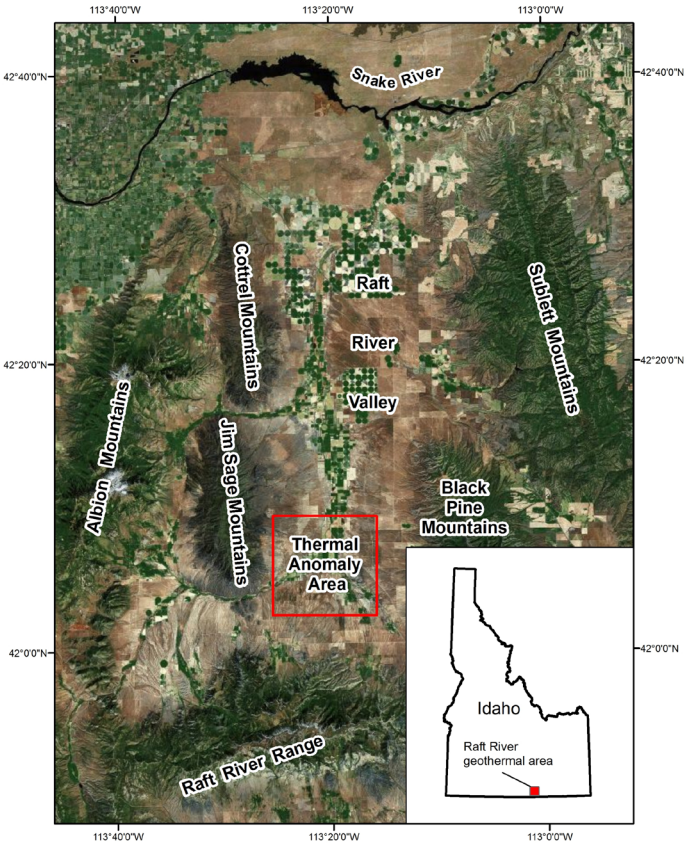

Figure 1. Location map.

National Laboratory for seismic monitoring, distributed temperature perturbation measurements, and electromagnetic surveys and by Sandia National Laboratories for televiewer surveys.

The primary objective of this project is to improve the performance of the Raft River geothermal production area by enhancing the permeability of well RRG-9, which is located to the south of the main production bore field. As part of this effort, new data, including X-ray diffraction, Bouguer corrected gravity, 3D magnetotelluric (MT), and drilling data and historical data including geologic maps have been added to a GIS database to facilitate visualization and analyses. This paper documents the results.

General Geology Overview

Lithology

The rocks in the area consists of generally denuded Archean and Proterozoic intrusives, schists, and quartzites, which are exposed in the Raft River and Albion Mountains, overlain with Miocene and Pliocene sedimentary, volcanic, and volcaniclastic rocks capped by younger sediments in the southern Raft River Basin. The borefield stratigraphic sequence follows from oldest to youngest.

Quartz Monzonite (adamellite): This rock, which is also found underlying much of the Raft River Mountains, has been described as mainly gneissose grading up-ward to schist (Compton et al, 1977). Wells (2001) describes the upper part of this unit (the Raft River shear zone (RRSZ)), as having fabrics that grade upwardly from granitoid to protomylonite, mylonite, and locally ultramylonite and phyllonite. This unit has yielded an Rb-Sr whole-rock minimum age of 2180 ± 190 Ma (Compton et al., 1977) from a sample taken in the northeastern Raft River Mountains in Clear Creek Canyon; however, its age is generally described, in various reports, as Archean.

Lower Narrows Schist (Proterozoic): This unit is a quartz, muscovite, biotite, chlorite schist that is cut by minor calcite and chlorite veins (Jones et al., 2011; Blackett and Kolesar, 1983).

Elba Quartzite (Proterozoic): This formation is generally a white ductilly-sheared metaquartzite that is commonly cross-bedded, locally green, and contains pebble beds. It is derived from a feldspathic sandstone protolith (Compton et al., 1977).

Upper Narrows Schist (Proterozoic): A ductilly-sheared quartz, K-feldspar, muscovite, biotite schist with minor chlorite veining and traces of calcite veins (Jones et al, 2011).

Quartzite of Yost (Proterozoic): A discontinuous white (green locally) thinly-bedded metaquartzite with muscovite (Jones et al, 2011; Compton et al, 1977).

Lower Tuffaceous Member (Salt Lake Fm - Miocene): Tuffaceous siltstones and poorly welded crystal-rich ash-flow tuffs with minor rhyolite flows (Jones et al., 2011).

Jim Sage Member (Salt Lake Fm – Late Miocene): Glassy to devitrified rhyolite flows that are often silicified in the upper part of the unit (Jones, 2011). Jim Sage Volcanic Member rocks in the Jim Sage and Cottrel Mountains were emplaced into their current location by late stage movement along the Raft River detachment fault.

Upper Tuffaceous Member (Salt Lake Fm) – Late Miocene/Pliocene): This unit consists of immature, poorly sorted, and poorly rounded sandstones, siltstones (often carbonate rich), and generally lithic and crystal-rich ash-flow tuffs (Jones, 2011).

Raft River Fm (Pliocene/Quaternary): Younger mixed sediments.

Structure

The regional structure is dominated by the Albion-Raft River-Grouse Creek metamorphic core complex and associated detachment faults separating ductilly deformed footwall shear zones from brittle hanging wall rocks. Covington (1983) inferred that up to a 10,000 m thickness of allochthonous Paleozoic and Mesozoic rock slices covered the entire area by the middle Oligocene. He further postulated that, by late Miocene, coherent gravity slide-blocks had moved about 25 km eastwardly, away from the Albion Mountains, along the Raft River detachment fault (RRDF). Malavieille (1987) invokes extensional tectonics as the catalyst of this movement. The spatial displacement is later corroborated by Wells (2001) who states that "mapping and strain and kinematic analysis indicate that the top-to-the-east Raft River shear zone initially developed parallel to an unconformity separating Archean rocks from overlying Proterozoic quartzite and schist for at least 24 km in the shear direction."

In the RRSZ, mylonitic fabrics are most highly developed in the Elba Quartzite and overlying schist, with this fabric being overprinted by cataclastic deformation upward toward the detachment fault (Wells et al., 2001). Coaxial flow has also affected the RRSZ causing thinning, which has been an important component of deformation (Compton, 1980; Wells, 2001; Sullivan, 2008). Additionally, it has been noted that strain associated with Tertiary extension quickly dies out in RRSZ Archean rocks beneath the Elba Quartzite and that the boundary between the two has acted as a strain-guide, concentrating Tertiary deformation within the quartzite (Sabisky, 1985; Malavieille, 1987a; Wells, 2001). This has obvious implications for enhanced geothermal system development.

Thermochronology indicates that the onset of motion along the RRDF began ~20-25 Ma and that movement ceased ~7.4 Ma (Wells et al., 2000). Over this time the RRSZ was unroofed creating the Raft River Basin. Now, only small remnant klippen remain on the east flank of the Albion Mountains and on the north and eastern flanks of the Raft River Mountains (Covington, 1983).

Within and near the thermal anomaly, recent extensional fault activity is marked by surface scarps. Seismic refraction and reflection data analyses indicate that these faults generally sole out into the RRDF (Ackerman, 1979; Covington, 1983). Mapped extensional fault zones in this area include the Horse Well and Bridge fault zones (Fig. 2). Late Miocene(?) dextral strike-slip faults have also been mapped: one offsetting the Cottrel and Jim Sage Mountains and the other at the southern margin of the Jim Sage Mountains (Fig. 2). These may be tear faults associated with the differential movement of these blocks along the RRDF.

Methodology — GIS Development

ArcGIS was used for the development of a geospatial database to facilitate data visualization and analysis to help achieve a better understating of the geology in the thermal anomaly area. The datasets developed using the GIS system included (1) point and line shapefiles showing well deviations; (2) a point lithologic shapefile containing formation top elevation values; (3) a min-

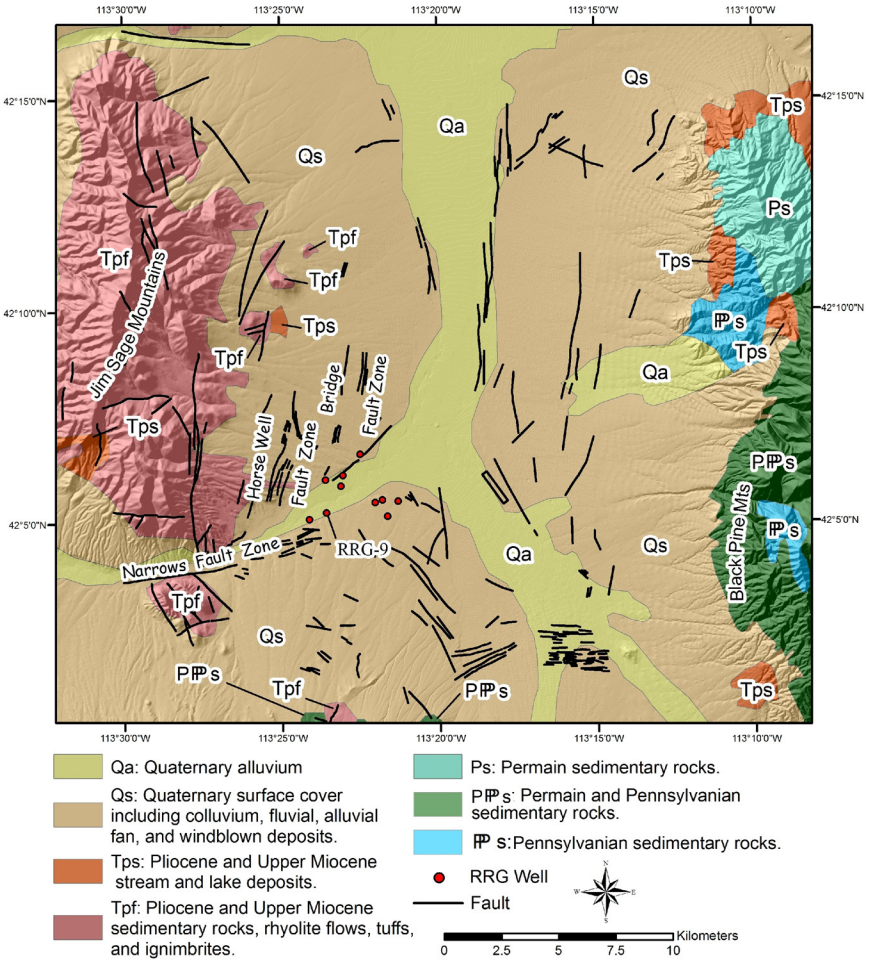

Figure 2. Surface geology map (after USGS, 2005; Link, 2002; Williams at al., 1974).

eralogic shapefile containing X-ray diffraction (XRD) data; (4) shapefiles containing faults interpreted from geophysical data; (5) surface geology shapefiles; (6) a raster Bouguer gravity image; and (7) several horizontal raster MT depth slices.

Wells, including deviations where applicable, were incorporated from well survey data as Z-aware points. The points were then converted to lines for use in 3D visualization in their proper spatial context using ArcScene (Fig. 3). The well point data were then used to extract XY coordinates for formation tops. XRD data XY coordinates were then associated with true vertical depths and elevations, derived from the well points, in a comma delimited text file which was used to generate new point shapefiles (Fig. 3).

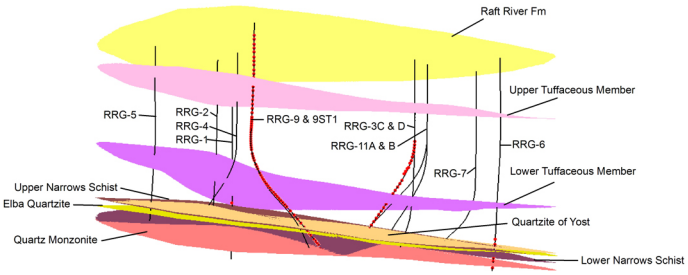

Figure 3. Wells, showing deviations where applicable, XRD data locations (red balls), and formation tops (variably colored surfaces).

The XRD shapefiles allow rapid query of down-hole mineralogic data to help determine hydrothermal alteration types per formation.

A lithology shapefile was then created. This was done by determining formation top depths from mud logs and associating these with appropriate points in a copy of the well dataset. The formation top data points were then used to create statistical surfaces using the *Interpolate* tool in the ArcGIS *Spatial Analysis* toolbox. The Spline-Tension method was used for this. The results can be seen in Figure 3.

The next task was to prepare datasets for use in creating geologic cross-sections. The first step was to extract formation top elevations, from the formation top statistical surfaces mentioned above, into shapefiles for use in creating digitizing templates. In preparation for the data extraction, polyline shapefiles were first made representing the paths of the cross-sections (see example on Fig. 4). New vertices were then added to the polylines at 20 foot intervals using the *Densify* tool in the *Editing* toolbox. The lines were then converted to points using the *Features Vertices to Points* tool in the *Data Management Tools* toolbox *Features* option. The point shapefiles were then used for the data extraction.

The data extraction was facilitated using the *Extraction* tool *Extract Multi Values to Points* option in the *Spatial Analyst Tools* toolbox. The shapefile tables, with the newly appended data, were then exported to comma delimited text files which were imported into Excel spreadsheets where they were

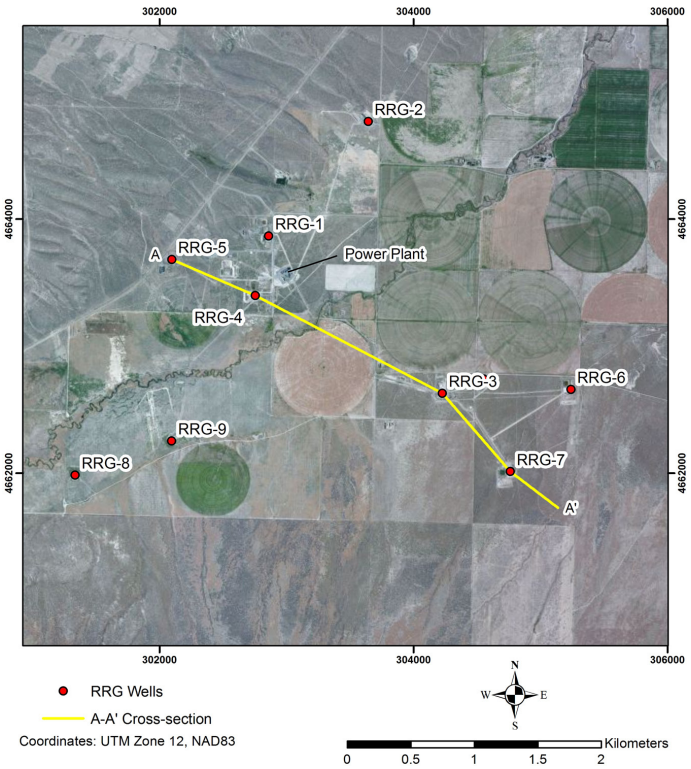

Figure 4. Cross-section line A-A′ shown in relation to RRG wells.

used to create line graphs (see example on Fig 5.). The line graphs were then converted into Tiff images, which were used as digitizing templates in ArcGIS.

A Tiff image can be used directly in ArcGIS and lithologic units digitized into a polygon shapefile. However, better results are achieved if a coordinate system is applied to the template image prior to digitizing. This can be accomplished using a world file. To create a world file, extreme upper-left pixel coordinates and the XY dimensions of the pixels must be determined.

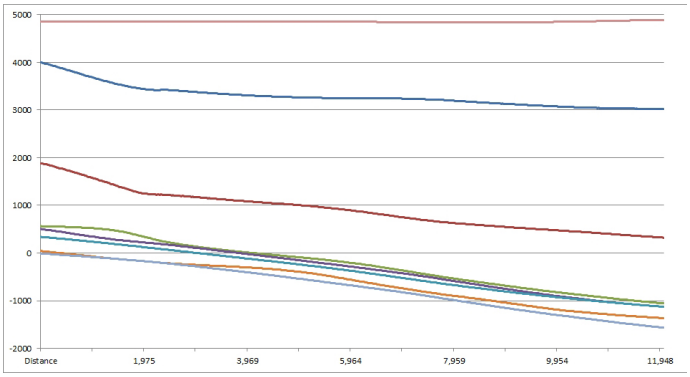

Figure 5. Formation tops template used to facilitate digitizing in ArcGIS for cross-section development. Each colored line represents a formation top with elevations values on the Y-axis and distance shown on the X-axis.

This info can be easily be calculated by comparing graph axes values with initial pixel screen values using ArcGIS. The upper-left pixel value is always initially 0,0 on the template image. Once this information is collected the world file is constructed using a text editor as follows:

5.5 (pixel width)
0.0 (rotation value – rarely used)
0.0 (rotation value – rarely used)
-5.0 (pixel height – value is always negative)
-55 (X coordinate)
5025 (Y coordinate)

Note: The bracketed comments are not included in the file and are shown only for clarification. Additionally, when first adding the template image to ArcGIS, the option of building pyramids will be given – pyramids are not built until the final file is created and applied.

To work properly the world file must be named correctly and be stored in the same folder as the image it applies to. The file name extension must always consist of the first and last letters of the raster file's extension followed by a "w." For example, for a raster image named AA_template.jpg, the world file would be named AA_template.jgw – for AA_template.tif, the world file would be named AA_template.tfw. Upon completion, a new map document is opened and the template image added. Accuracy is checked by placing the cursor on graph axes values. If accuracy is not as expected, pixel XY dimension values in the world file can be adjusted slightly to achieve near perfect results. Digitizing in ArcGIS works better when there is a coordinate system and, as an added bonus, accurate measurements can be made on the template to help facilitate the placement of features such as wells and faults.

A lithologic contact shapefile is then made and new field added to its table to accommodate a description that will be used to automate the creation of a legend. Polygons are then digitized into this file using the template as a guide. Wells and faults can also be added to the cross-section as graphics and lithologic polygons can be edited as necessary to represent rock offset along faults. After the polygons are symbolized, a legend can be added.

Finally, a second template is created in Excel with no formation top lines. This is used to replace the original in ArcGIS so that axes and axes values are shown with no other graphics. However, before adding this, the original world file is copied and renamed to match the name of this this new image. Figure 6 depicts one of the cross-sections made for this project using the above method.

To continue GIS geodatabase development, faults were mapped from the Bouguer corrected gravity image and the 3D MT data slices. Initial fault locations were picked using five 2D gravity profiles by geophysicist Howard Ross, Ph.D. (Pers. Comm.). These picks were expanded using the *3D Analyst* in ArcGIS. The *3D Analyst > Interpolate Line* tool, coupled with the *Profile Graph Tool*, facilitates the rapid generation of 2D gravity profiles. Points of inflection can be located and then queried for location on the gravity image plan view aiding in fault mapping (Fig. 7). MT data depth slices (Fig. 8) were then used to help constrain fault depths and to map additional faults.

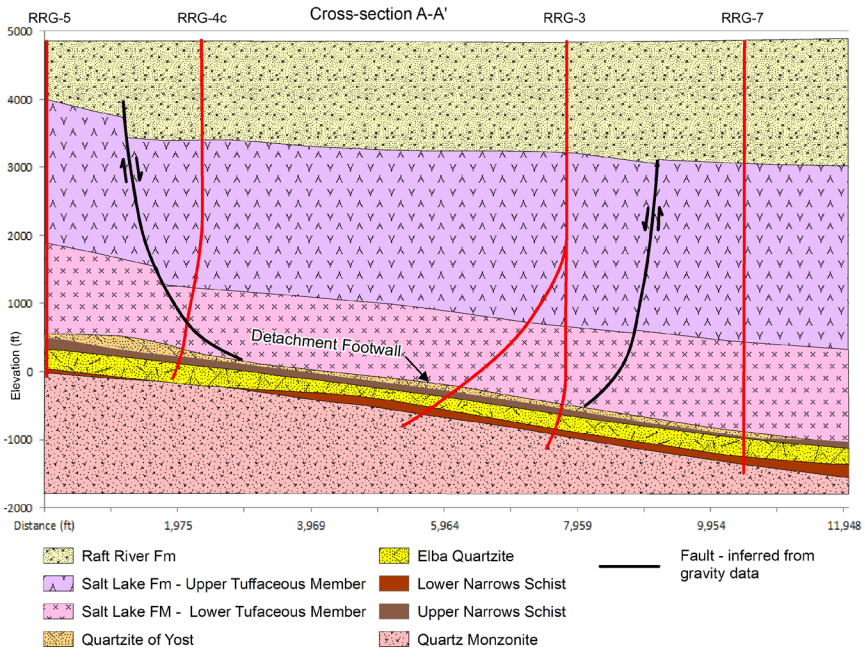

Figure 6. Cross-section A-A′ (see Fig. 4 for orientation).

Discussion

GIS is an excellent resource for the visualization, interpretation, and distribution of geological and geophysical data. But, perhaps an even more significant value is the opportunity GIS affords, during various stages of processing, to review and understand data better.

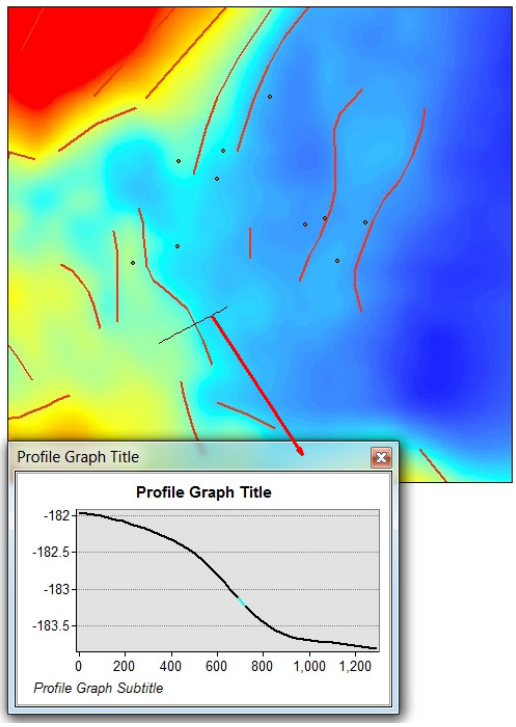

Figure 7. Gravity profiles generated using the ArcGIS 3D analyst aid in fault mapping. Faults are depicted as red lines.

For example, the lithologic data shown in Figures 5 & 6 indicates that all formation tops dip gently to the east. This is in response to the eastward dipping detachment surface that controls the Raft River basin. Although a simple observation, this will aide in future well targeting and GIS facilitated the necessary visualization in an effective manner.

Additionally, for this project, a good understanding of the geologic structure in the study area was a priority. The ability to visualize geophysical data and efficiently map faults, using tools found in ArcGIS as an aid, helped develop this understanding. For instance, faults mapped from gravity data in the Bridge Fault Zone area generally strike NNE (Figs. 7 & 9), which agrees with those mapped in many previous studies. There are also geologically recent surface scarps in this area suggesting that this system is relatively young and related to the modern extensional stress fields. However, NNW-NW trending faults, inferred from MT data (Figs, 10 & 11), further complicate the structure.

The NW-NNW striking faults may have originated from R' shear related to the Narrows dextral strike-slip fault zone under different stress-fields, perhaps in the late Miocene. Well RRG-4, currently the most prolific well in the field, is juxtaposed to a NW striking fault inferred from MT data (Fig. 11) and a NNE striking normal fault that may be part of the southern extension of the Bridge zone. Interestingly, stimulation of this well produced a fracture that was oriented approximately E-W (Campbell et al.,

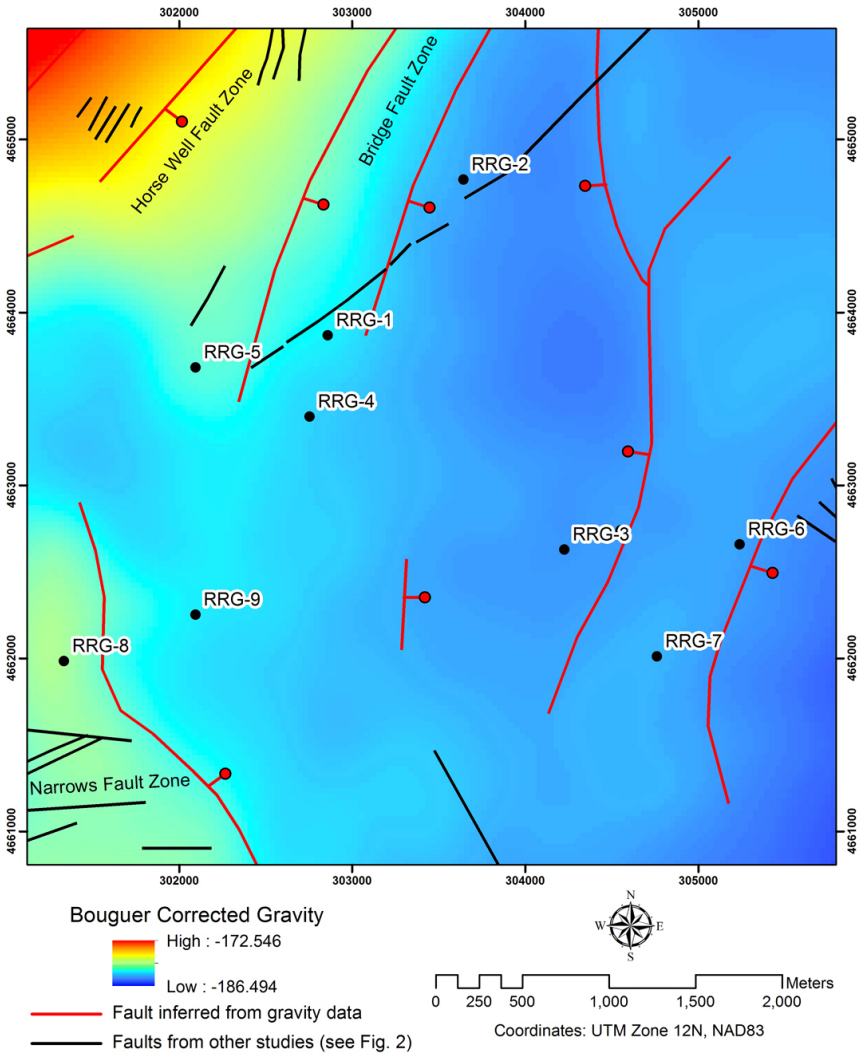

Figure 9. Bouguer corrected gravity image with faults. Note the general NNE trend of most faults inferred from gravity. Additionally, a comparatively minor anomaly exists between faults near RRG-3 and RRG-6. This could permissively represent a glide-block that has moved partially down the RRFZ or an area of silicification associated with fault controlled hydrothermal fluids.

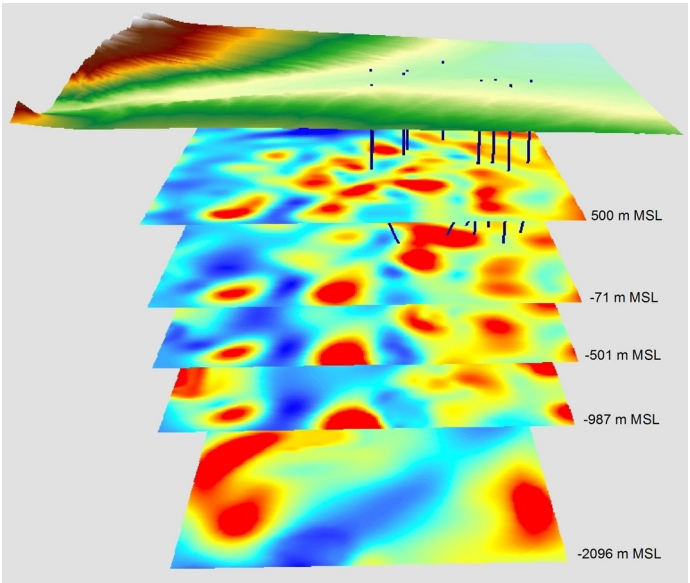

Figure 8. Magnetotelluric data slices, at various depths, shown in relation to the Earth's surface.

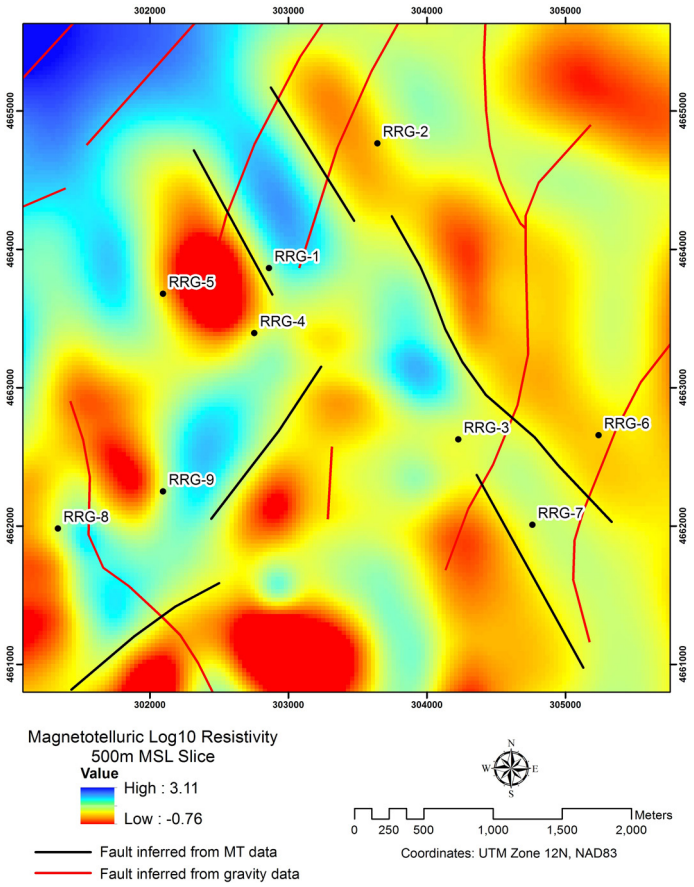

Figure 10. Magnetotelluric slice at 500m elevation. The east half of this slice lies in the Upper Tufaceous Member with the western half cutting into the Lower Tufaceous member. Most conductive areas are likely related to hydrothermal alteration of volcanic and volcaniclastic rocks above the geothermal reservoir. Some faults are suggested by the data and these are only partially on trend with faults mapped from gravity data or surface escarpments. RRG wells are added as geographic reference.

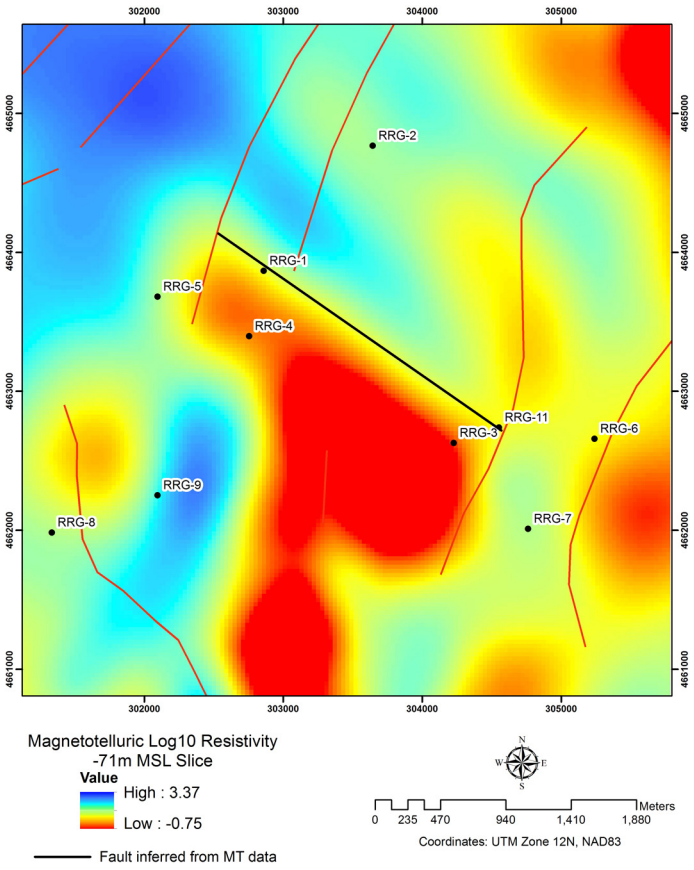

1981), while the stimulation of well RRG-5 produced a NE-SW trending fracture (Campbell et al., 1981). Televiewer data taken in well RRG-9ST1, as part of this project, also reveals stimulation fractures that generally strike NNE-SSW. The fractures in RRG-5 and RRG-9ST1 are close to what would be expected considering that the current least horizontal stress is normal to the strike of the NNE trending younger faults in the Horse Well and Bridge fault zones. However, the fracture orientation in well RRG-4 may be, in part, due to initial stresses related to those which produced Ridel shear in the area. Additionally, this area may have undergone a period of transtension.

However, faults mapped in previous studies (Fig. 2) and those inferred from gravity data (Fig. 7) south of the Narrows fault zone are generally are oriented NNW, with a notable departure to the eastward strike of a fault swarm that is seen in the southeastern corner of Figure 2. When considering fault geometries in this area, the angular relationships suggest Riedel shear patterns. This would suppose that that the stress fields that produced the Riedel shear are still controlling the local structure, that the principal displacement zone would be the Narrows fault system, and that this system may have been active in the geologic recent. If this is the case, a NNE trending fault swarm, immediately west of the above mentioned east-striking system, could represent P-shear. However, the strike of these faults appears to be generally parallel with the Narrows fault system raising the possibility of releasing right step-over with associated extensional duplex development. This could explain the presence of some of the NNW trending faults. Considering the scale of previous mapping and potential for spatial error propagation during drafting and digitization, neither of these possibilities can be ruled out.

For further consideration, additional MT data depth slices and faults mapped from both MT and gravity data are shown on Figures 12-14 for comparison. There is, however, generally little spatial correlation between faults mapped from gravity and MT data. This may be explained by the shallow nature of the normal faults controlled by the current stress regime, which, as noted earlier, is corroborated by earlier studies using seismic data. Therefore, faults inferred from gravity data, but not seen in MT data at depths below the RRSZ, are believed to sole-out at the surface of the

Figure 11. Magnetotelluric data slice at -71m elevation. The eastern part of this image is associated with Lower Tuffaceous Member while the western half is primarily associated with rock in the RRSZ. There is little agreement between faults mapped from MT and gravity data. However, the black SSW trending fault immediately to the right of RRG-4 could be a continuation of the red fault located just to the left of RRG-2 – perhaps a less active segment. The NW striking fault running between RRG-3 and RRG-1 and its juxtaposition with faults interpreted from gravity may have implications for well productivity -- RRG-4 is the most prolific well in the field. This may be an R′ shear related to the dextral Narrows strike-slip fault system.

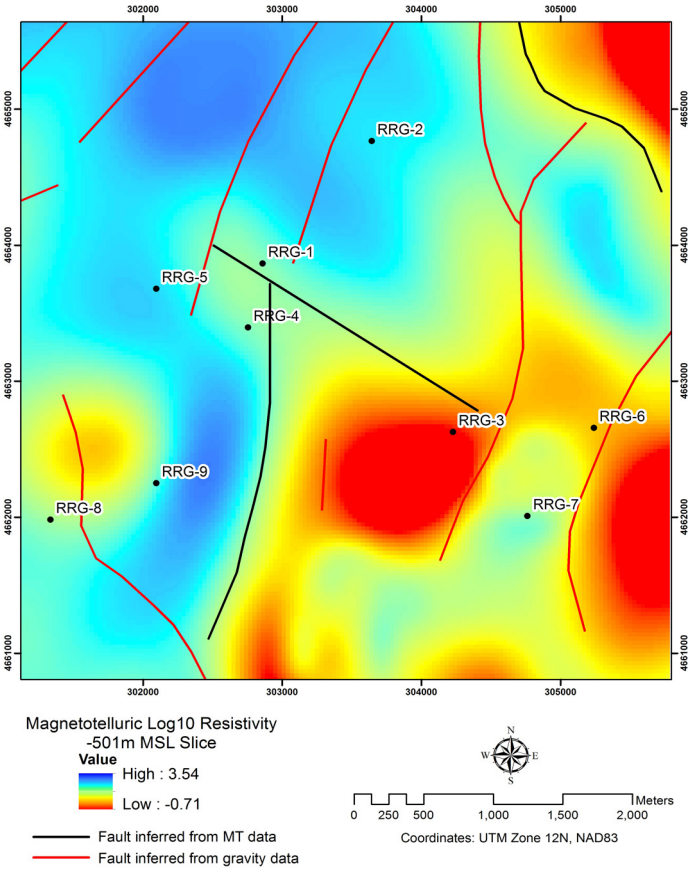

Figure 12. Magnetotelluric slice at -501m elevation. This entire slice is located at an elevation below the RRSZ, except perhaps along the eastern margin of the image. Faults inferred from the -71m elevation slice (Fig. 11) still appear generally valid on this slice although the anomalies are more subtle. Conductive zones in the lower-right part of the image have good spatial correlation with southern reach of two red (gravity inferred) faults in the southeastern quadrant of the image.

RRSZ as illustrated in Figure 6. MT slices in the basement show decreasing conductivity with depth (Figs. 13 and 14).

Finally, Ayling et al. (2011) classifies groundwater in the study area into four groups by chemistry including Groundwater Group 1, Groundwater Group 2, Deep Geothermal SE, and Deep Geothermal NW, with the Narrows fault zone separating the two deep geothermal groups. Groundwater Group 1 flows generally unencumbered from the NW to SE through the shallow Raft River Fm, while Groundwater Group 2 flows from SE to NW through the Salt Lake Fm at depth to an area between RRG-1 and RRG-5 and then reverses directions flowing at a shallower level near the contact of the Salt Lake and Raft River Fms back to the SE. A NE striking normal fault, inferred from gravity data, in the Bridge fault zone can be seen cutting just to the east of RRG-5 on Fig. 9. This structure may function as an aquitard and be responsible for the flow reversal. The hydrologic reversal takes place in relatively young rocks that are not optimally indurated, where even moderate fault motion could permissibly create a significant clay (gouge) barrier to flow.

Conclusions

The GIS platform allowed the successful incorporation of numerous disparate datasets ranging from scanned geologic maps to numeric tabular data sets through the creation of both vector and raster datasets. It facilitated both 2D and 3D visualization of the data and the query of data in its proper spatial context. For example, the XRD data can be queried down-hole to determine if hydrothermal alteration exists within a rock unit and, if so, what type.

GIS was also very useful in developing geologic cross-sections. Specific tools in ArcGIS allowed data to be extracted and imported into Excel for template development. The templates were then used in ArcGIS to facilitate the digitizing of data. This helped relate faults to existing wells and will be useful in siting new wells in the future.

The visualization of gravity and magnetotelluric data, and the use of tools built into the GIS, effectively facilitated fault mapping. The Raft River thermal anomaly has a complex Miocene through Holocene structural history. Young NNE striking normal faults, north of the Narrows fault zone, are likely controlled by the current stress fields. However, these overprint possible R' faults,

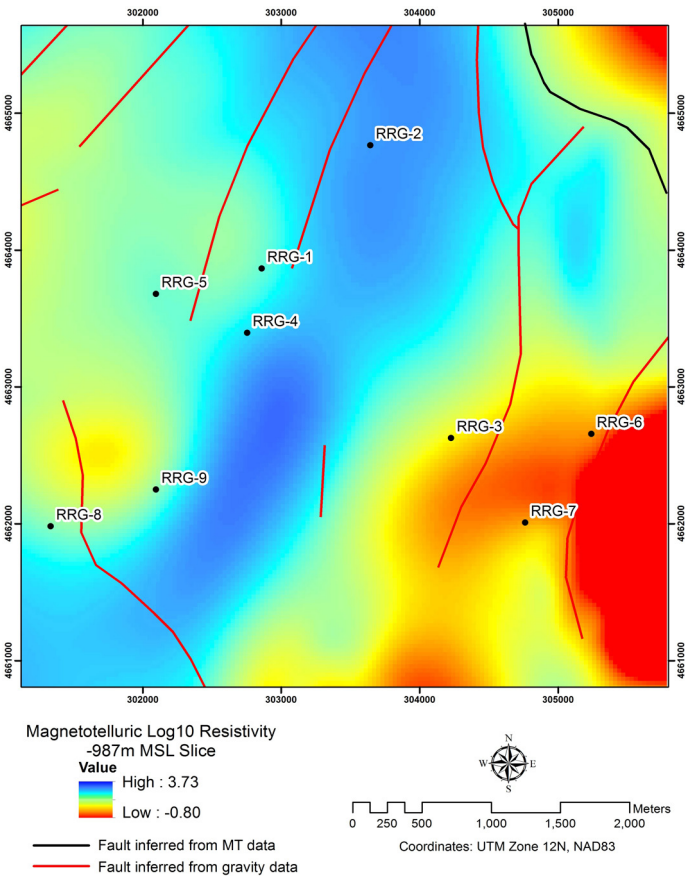

Figure 13. Magnetotelluric slice at -987m elevation. The rock represented in this dataset lies well into the basement below the RFSZ. The conductive anomalies that suggested structural control at shallower depths have mostly disappeared at this depth. A significant departure from this can be seen in the upper-right corner of the image and there is an enlargement of the conductive zone in the lower-right part of the image. An enlarging area of resistant rocks also appears in the western part of the image.

that were mapped from MT data, which would have originated under different stress fields in the relatively recent geologic past. Well stimulation in this area generally produces NNE oriented fractures that, along with NNE trending young faults, indicate that the least horizontal stress is SSE-NNW. However, stimulation of well RRG-4 produced east-west oriented fractures that may be related to the older stress fields which produced faults related to Riedel shear.

The comparison of gravity and MT data indicates that most faults do not have offsets that penetrate beneath Cenezoic fill. This is corroborated by earlier seismic studies (Ackerman, 1979; Covington, 1983). South of the Narrows fault zone NNW, NNE, and E striking fault zones may have developed as Riedel shears and the stress fields here may still reflect this. Additionally, a set of ENE trending faults, approximately parallel to and southeast of the Narrows fault zone, may indicate a right step-over which opens the possibility of extensional pull-apart development. The structural complexity in the study area is also facilitating ground water and geothermal fluid compartmentalization which can be explained by fault orientations.

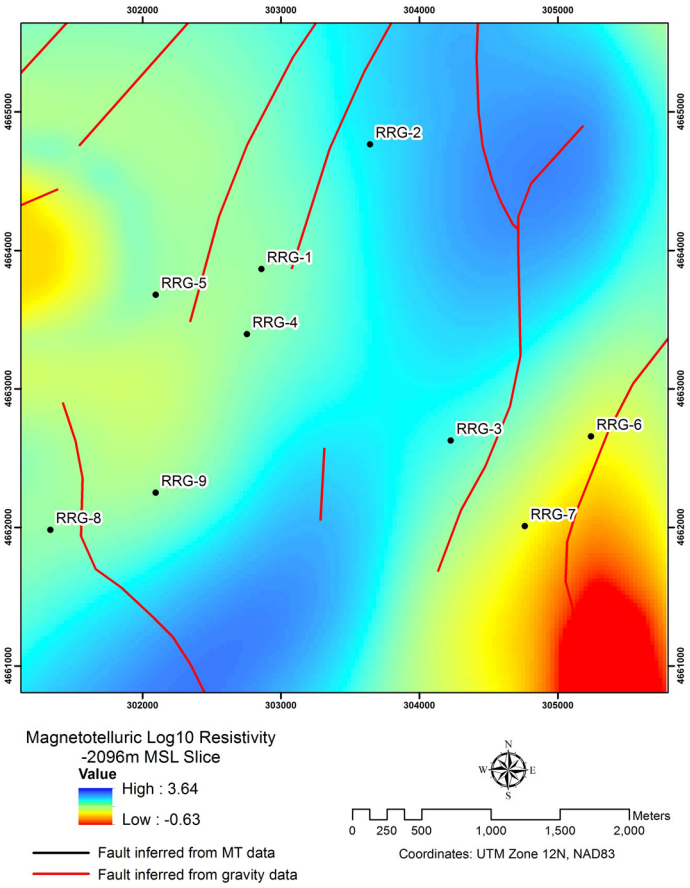

Figure 14. Magnetotelluric slice at -2096. The deepest slice reveals a general pattern of increasing rock resistance.

References

Ackerman, H. D., 1979. Seismic refraction study of the Raft River geothermal area, Idaho, *Geophysics*, v. 44, no.2, p. 216-225.

Ayling, B., P. Molling, R. Nye, and J. Moore, 2011. Fluid geochemistry at the Raft River geothermal field, Idaho: New data and hydrogeological implications, *Proceedings*: Thirty-Sixth Workshop on Geothermal Reservoir Engineering, Stanford University, SGP-TR-191.

Blackett, R. E., and P. T. Kolesar, 1983. Geology and alteration of the Raft River geothe4rmal systems. Idaho, Geothermal Resources Council *Transactions*, v. 7, p. 123-127.

Cambell, D, R. J. Hanold, A. R Sinclair, and O. J. Vetter, 1981. A Review of the geothermal reservoir well stimulation program, International Geothermal Drilling and completion Technology Conference, Albuquerque, NM, 17 p.

Compton, R.R., 1972. "Geologic map of the Yost quadrangle, Box Elder County, Utah and Cassia County, Idaho." US Geologic Survey Miscellaneous Investigation Map I-672, scale 1:31,680.

Compton, R.R., 1975. "Geologic map of the Park Valley quadrangle, Box Elder County, Utah and Cassia County, Idaho." US Geologic Survey Miscellaneous Investigation Map I-873, scale 1:31,680.

Compton, R.R., Todd, V.R., Zartman, R.E., Naeser, C.W., 1977. "Oligocene and Miocene metamorphism, folding, and low angle faulting in northwest Utah." Geological Society of America *Bulletin 88*, p. 1237-1250.

Compton, R.R., 1980. "Fabrics and strains in quartzites of a metamorphic core complex, Raft River Mountains, Utah." *in* Crittenden, M.D. Jr., et al., eds., Cordilleran Metamorphic Core Complexes: Geological Society of America *Memoir 153*, p. 385–398.

Covington, H. R., 1983. "Structural evolution of the Raft River Basin, Idaho." Geological Society of America *Memoir 157*, p. 229-237.

Jones, C, J. Moore, W. Teplow, and S. Craig, 2011. Geology and hydrothermal alteration of the Raft River geothermal system, Idaho, *Proceedings*, Thirty-Sixth Workshop on Geothermal Reservoir Engineering, Stanford University, Stanford CA., SGP-TR-191.

Link, P. K., 2002. Cassia County, ID, geologic map, Digital Atlas of Idaho, Idaho State University, Geosciences Department.

Malavieille, J., 1987. "Extensional shearing deformation and kilometer-scale "a"-type folds in a cordilleran metamorphic core complex (Raft River Mountains, northwest Utah)." *Tectonics*, v. 6, p. 423–448.

Sullivan, W.A., 2008. "Significance of transport-parallel strain variations in part of the raft river shear zone, Raft River Mountains, Utah, USA." *Journal of Structural Geology*, v. 30, p. 138–158.

USGS NR_GEO, 2005, A spatial database for the geology of the Northern Rocky Mountains - Idaho, Montana, and Washington, *Edition:* 1.0, Open-File Report 2005-1235, U.S. Geological Survey, Menlo Park, California.

Wells, M.L., 2001. "Rheological control on the initial geometry of the Raft River detachment fault and shear zone, western United States." *Tectonics,* v. 20, p. 435-457.

Wells, M. L, L. W. Snee, A. E. Blythe, 2000. "Dating of major normal fault systems using thermochronology: An example from the Raft River detachment, Basin and Range, western United States." *Journal of Geophysical Research*, v. 105, no. B7. p. 16,303–16,327.

Williams, P. L., K, L, Pierce, D, H, McIntire, and P. W. Schmidt, 1974. Preliminary geologic map of the southern Raft River area, U.S.G.S. Open File Report, 1:24,000.